Article

An Accessible Yarn-Based Sensor for In-Field Detection of Succinylcholine Poisoning

Victor Ong [1] [iD]**, Nicholas R. Cortez** [2]**, Ziru Xu** [1]**, Farbod Amirghasemi** [1] [iD]**, Mohamed K. Abd El-Rahman** [3,4] **and Maral P. S. Mousavi** [1,*] [iD]

1   Department of Biomedical Engineering, University of Southern California, 1042 Downey Way, Los Angeles, CA 90089, USA
2   Department of Biological Sciences, University of Southern California, Allan Hancock Foundation Building, Los Angeles, CA 90089, USA
3   Analytical Chemistry Department, Faculty of Pharmacy, Cairo University, Kasr-El Aini Street, Cairo 11562, Egypt
4   Department of Chemistry and Chemical Biology, Harvard University, 12 Oxford Street, Cambridge, MA 02138, USA
*   Correspondence: mousavi.maral@usc.edu

Abstract: Succinylcholine (SUX) is a clinical anesthetic that induces temporary paralysis and is degraded by endogenous enzymes within the body. In high doses and without respiratory support, it results in rapid and untraceable death by asphyxiation. A potentiometric thread-based method was developed for the in-field and rapid detection of SUX for forensic use. We fabricated the first solid-contact SUX ion-selective electrodes from cotton yarn, a carbon black ink, and a polymeric ion-selective membrane. The electrodes could selectively measure SUX in a linear range of 1 mM to 4.3 µM in urine, with a Nernstian slope of 27.6 mV/decade. Our compact and portable yarn-based SUX sensors achieved 94.1% recovery at low concentrations, demonstrating feasibility in real-world applications. While other challenges remain, the development of a thread-based ion-selective electrode for SUX detection shows that it is possible to detect this poison in urine and paves the way for other low-cost, rapid forensic diagnostic devices.

Keywords: electrochemical sensors; on-site testing; electrochemistry; potentiometric electrodes; low-cost devices; thread-based electrodes; forensics; yarn-based sensors

1. Introduction

Succinylcholine (SUX) is a common clinical anesthetic used worldwide [1–3]. It is an analog to acetylcholine, an important neurotransmitter responsible for muscle movement [4]. SUX competitively binds to acetylcholine receptor sites in neurons and induces prolonged neuron polarization, preventing action potential transmission between neurons and inducing short-term paralysis [5,6]. Butyrylcholinesterase (BChE, also known as pseudocholinesterase) is an endogenous nonspecific cholinesterase that degrades SUX into choline and succinylmonocholine, which BChE again metabolizes into choline and succinate [6–8]. Degradation of SUX by BChE occurs on the order of minutes and is therefore a choice drug for surgical anesthesia [2,9,10]. However, patients must be placed on respiratory support, and in patients with deficient BChE activity, SUX can induce prolonged apnea and death by respiratory paralysis [5,6]. Outside the clinic, the drug's fast paralytic action, endogenous degradation, and inconspicuous metabolic products have earned it an infamous reputation as the "untraceable poison" [8,11–13]. It was used in the high-profile murder cases of William Farber, Kathy Augustin, and a serial murder case in Japan [14]. The 1981 murder of Shannon Mohr reached the greatest notoriety, spawning the 1993 movie, "Victim of Love: The Shannon Mohr Story".

There is currently no simple field test to detect SUX poisoning in victims of homicide or attempted homicide. Current forensic techniques for SUX detection, such as high

performance liquid chromatography (HPLC) and mass spectrum (MS) analysis, require time-consuming, expensive, and elaborate laboratory tests [2,3,9–12]. Because the samples require transport, cholinesterase inhibitors need to be added to prevent rapid SUX degradation in blood [7,12]. While alternative matrices (such as urine) may show advantages over blood, it remains that laboratory tests such as HPLC, MS, and thin layer and gas chromatography require a large resource commitment [15]. It takes significant time, resources, skilled personnel, and facilities to preserve, transport, prepare, work up, and analyze biological SUX samples. This lengthy process can hinder criminal investigations and be inaccurate due to the endogenous degradation of SUX. Therefore, this work aims to develop a rapid and accessible electrochemical sensing platform for detecting SUX in the biofluids of victims.

Electrochemical analysis is fast, accurate, typically label-free, and requires significantly less complex equipment than optical, chromatographic, and MS techniques. Electrochemical sensors are typically comprised of electrodes immersed in solution and connected to an electrochemical workstation. Recent advances in the field focus on developing smaller and more robust electrodes [16–26]. The past decade has yielded great success in the development of electrochemical sensors for clinical analysis, using low-cost and ubiquitous materials such as paper, fabrics, threads, and thin polymer films [20,25–33]. Devices such as these have been used to detect blood glucose levels, diabetes biomarkers, bacterial infection, mercury, and breath humidity, among other things [26,27,29,32,34–37]. Yarn-based sensors are particularly exciting due to their flexibility, durability, ease of storage, and natural microfluidic properties. Recent work has used yarn as the basis of electrochemical sensors, significantly reducing overall cost and improving durability and accessibility [20,25,26,30,31,33,38]. These include cotton-based batteries, sweat-sensing electrodes, and sensors for urea, cortisol, glucose, trimethylamine, and acetylcholine [25,26,30,31,33,38,39].

This work utilizes the permanent positive charge of SUX to develop an electrochemical SUX sensor based on potentiometric ion sensing. Potentiometry is an electrochemical measurement that is particularly attractive for quantifying the presence of an ion in solution. It is low-power (does not require pushing a current), can be highly selective for a target ion, and has a millisecond response time [40,41]. Inner filling solution-based potentiometric sensors have been well-established, but because they require stable liquid–solid interfaces, they are difficult to miniaturize [40,42]. Relatively recent advances in the field have brought the advent of solid-contact potentiometry, which eschews the liquid–solid interface of the inner filling solution-based potentiometric sensor [16,18–22,43–47]. Yarn-based solid-contact potentiometric sensors have been developed previously for the detection of electrolytes [20].

In this work, we have developed the first thread-based ion-selective electrode (ISE) for quantifying SUX in the urine of homicide and attempted homicide victims (Figure 1). Previous work has established the detection of acetylcholine and choline with potentiometry and the viability of a yarn-based solid-contact electrode [20,39,48]. Further, electrochemical sensors for fentanyl, cocaine, heroin, ketamine, and other illicit drugs have been developed [17,23,49–53]. Urine contains higher levels of SUX compared to blood because the latter contains BChE, which continues to degrade SUX, while urine does not [7]. The sensors developed in this work would allow detectives to perform rapid field tests for SUX residue for evidence collection and make informed determinations if more complex tests are warranted. These field tests would also serve as an early-detection device in the event that samples decompose during storage and transport to a forensic laboratory. To the best of our knowledge, this work presents the first yarn-based potentiometric sensor for the detection of SUX and the first SUX sensor capable of accessible on-site detection of SUX in urine.
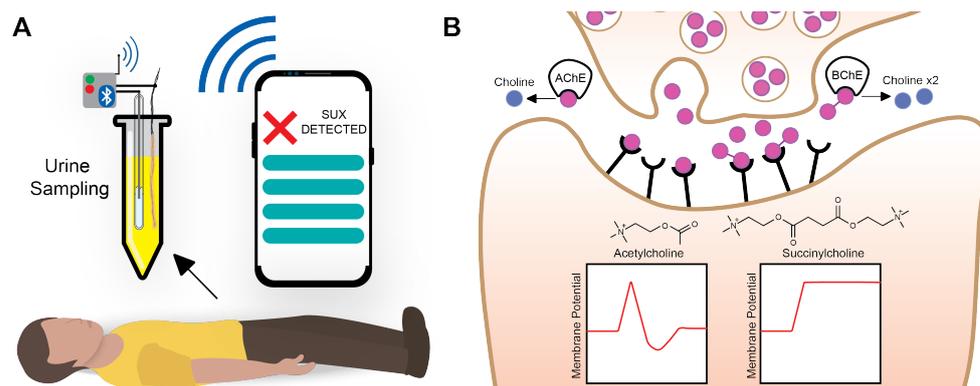
Figure 1. (**A**) At the scene of an investigation or during an autopsy, a urine sample can be obtained via a catheter or syringe and deposited into a container. The proposed thread-based ISEs can be placed into the urine with a reference electrode and wireless transducer to perform readout to a smartphone. A simple app can be coded to display the positive/negative presence of SUX, the concentration of SUX, and more detailed information about the device calibration and current *emf* reading. (**B**) The biological mechanism of SUX action. The dimer outcompetes acetylcholine for receptor sites and causes prolonged polarization of the neuron, leading to paralysis [5].

2. Materials and Methods

2.1. Materials and Reagents

Poly(vinyl chloride) (PVC), calix[4]arene-25,26,27,28-tetrol (CX4), calix[6]arene (CX6), 2-nitrophenyl octyl ether (NPoE), succinylcholine chloride (SUXCl$_2$) dihydrate, sodium chloride (NaCl), and a platinum (Pt) reference electrode were obtained from Sigma-Aldrich (St. Louis, MI, USA). Sodium tetrakis(3,5-bis(trifluoromethyl)phenyl)borate (NaTFPB) was purchased from ASTA Tech (Bristol, PA, USA).

Silver (Ag) wire and calcium chloride (CaCl$_2$) were obtained from Beantown Chemical (Hudson, NH, USA). Potassium chloride (KCl), magnesium chloride (MgCl$_2$), hydrochloric acid (HCl), tetrahydrofuran (THF), and human pooled urine were obtained from Avantor (Radnor, PA, USA). Ammonium chloride (NH$_4$Cl) was sourced from MP Biomedicals (Santa Ana, CA, USA).

We used a three-electrode cell to coat the silver wire with silver chloride. We applied a current density of 0.4 mA/cm^2 in 0.1 M HCl solution for 30 min on a CH Instruments (Austin, TX, USA) electrochemical workstation. Tygon tubing (0.25 inch diameter) was obtained from Saint-Gobain (Courbevoie, France), and a double-junction reference electrode was sourced from Mettler Toledo (Columbus, OH, USA). An EMF 16 electrochemistry interface from Lawson Labs (Malvern, PA, USA) was used in conjunction with the EMFSuite v1.03 software by Fluorous Innovations (St. Paul, MN, USA). Ultrapure water (DI water) was used throughout the experiments. Yarn-based electrodes were developed with Aunt Lydia's Fashion Size 3 yarn (Amazon.com), VXC72 carbon black (CB) (Cabot), and THF.

2.2. Fabrication of Conventional ISEs for SUX

To develop conventional ISE for SUX, ion-selective membranes (ISM) were used to select for SUX over other positively-charged ions. An ISM cocktail was created by dissolving 330 mg PVC, 660 mg NPoE, 5.1 mg CX4 (or 7.6 mg CX6), and 4.9 mg NaTFPB into 2.5 mL THF and stirring overnight. The next day, the membrane was cast by pouring the ISM cocktail into the bottom of a petri dish, taking care to avoid the formation of bubbles, then covered with the top of the petri dish. The petri dish was not air-sealed, allowing the THF solvent to evaporate slowly, yielding a 200 μm thick ISM. The ISM was cut into 3/7 inch diameter circles, and a 5-cm length of Tygon tube was cut. We added minimal THF to one end of the Tygon tubes and placed the circular CX4-ISMs on these ends, applying pressure. Because both the CX4-ISMs and Tygon tubes are soluble in THF, as the solvent dries, they bond together, forming the body of the electrode.

The electrodes were filled with an aqueous 100 µM SUXCl$_2$ and 20 mM KCl inner filling solution and sealed with parafilm. To complete the electrical connection, the AgCl side of an Ag/AgCl wire was inserted through the parafilm into the inner filling solution, and another layer of parafilm was added to secure the wire.

The electrodes were conditioned by immersing the sensing portion (membrane side) of the ISEs into a 100 µM aqueous SUXCl$_2$ solution and stirring gently overnight. This facilitates the exchange of the ionic site's sodium counterion with SUX, establishing a common chemical species between the sample solution and ISM. When not in use, the electrodes were stored by immersing the membrane portion into 100 µM aqueous SUXCl$_2$ solution.

2.3. Fabrication of Thread-Based ISEs for SUX

An ISM cocktail was prepared in the same fashion as for the conventional ISEs, except 100 µL of 0.1 M SUXCl$_2$ was added into the ISM solution while stirring overnight (Figure 2). This eliminates the later conditioning step by exchanging the sodium counterion found in the ionic site with SUX. This is important for thread-based ISEs, as they are designed for point-of-care applications, where conditioning the electrodes before measurement is not feasible. After adding the SUXCl$_2$, the ISM cocktail became cloudy, indicating the exchange of the sodium cation with the SUX cation and the precipitation of NaCl. The ISM cocktail was kept in a 1.7 mL Eppendorf tube to prevent solvent evaporation.
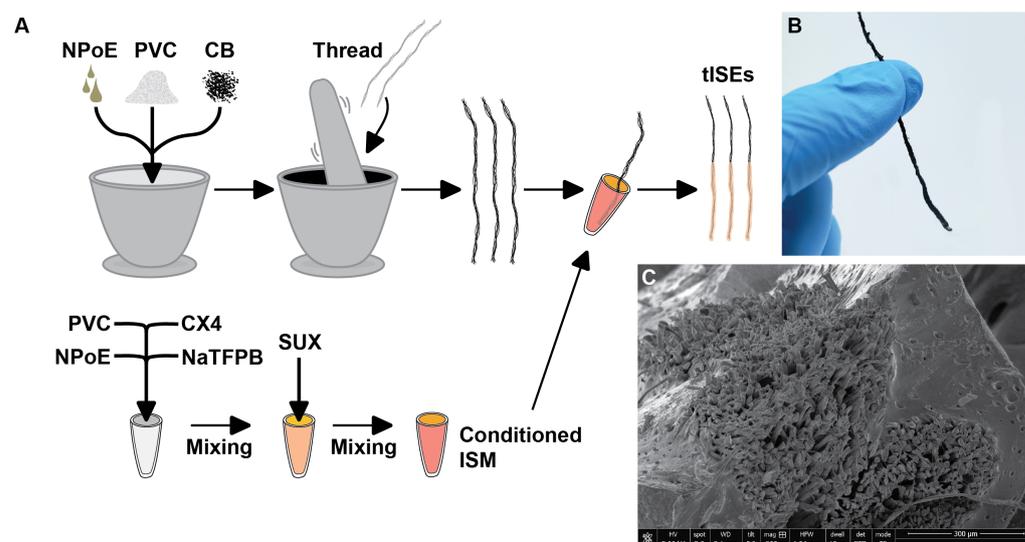

Figure 2. (**A**) The fabrication of the thread-based ISEs. The polymer support (PVC), plasticizer (NPoE), and carbon black (CB) were mixed using a mortar and pestle and deposited onto thread to make the thread-based conductive electrodes. The electrode was then dipped into the sensing cocktail to form the SUX-sensing membrane on the electrodes. (**B**) shows a fully-fabricated thread-based ISE, and (**C**) shows the SEM image of the cross-section of thread-based ISE. The smooth membrane coats the microscopic fibers.

Conductive ink was created by aggressively mixing 250 mg PVC, 500 mg NPoE, and 250 mg CB in 2.5 mL THF with a mortar and pestle (Figure 2). After 30 s, a length of yarn was added to the ink slurry while mixing continued. If the ink dried too quickly, 1 mL THF was added to solvate the dried ink for yarn uptake. The yarn electrodes were hung and dried overnight. The next day, one end of the electrodes was dipped into the ISM cocktail two times to create an even coating of ISM and allowed to dry. When not in use, the thread-based ISEs were rinsed with DI water and stored dry.

2.4. Calibration Curves and Selectivity Studies

Electrodes were connected to an EMF 16 potentiostat and data were collected with the EMFSuite software. A double-junction Ag/AgCl/Cl reference electrode with 3 M KCl

bridge electrolyte was used as a reference electrode [40]. We performed drift analysis by immersing fresh sensors into 1 mM SUXCl$_2$ solution for 30 min and recording emf (electromotive force). Drift is calculated as $\Delta\,emf$ per minute.

Calibration curves for SUX were obtained by performing either serial dilutions with deionized water (SUX calibration) or standard additions (interference measurements). The range covered 1 mM SUX and decreased until the sensor response became non-linear, typically around the 10 nM SUX range. For conventional ISEs, approximately 1 cm of clearance was allowed between the beaker and ISM to prevent the blockage of mass transport. For thread-based ISEs, we ensured that only the membrane portion was immersed into solution and was positioned 0.5–1 cm away from the beaker walls and bottom. We stirred the solution for 30 s after each dilution and waited 2 min before recording the average emf value over a 10-s interval. Two minute sampling time was selected arbitrarily to allow sufficient time for pipetting and solution exchange in a consistent manner, while still allowing for a rapid on-site analysis.

Interference tests and selectivity studies were performed with the fixed interference method. Electrodes were placed into a high background concentration of interfering ions and known amounts of SUX were spiked into the solution and stirred. Interference testing was performed in background concentrations of 100 mM KCl, 100 mM NaCl, 100 mM NH$_4$Cl, 100 mM CaCl$_2$, and 100 mM MgCl$_2$, and 20% urine.

Urine is a complex matrix containing many potentially interfering molecules. The performance of the electrodes was evaluated in urine to capture the overall impact that these interfering molecules would have on the sensors. We diluted our stock of urine fivefold to conserve our samples for all validation studies. Future miniaturization of the reference electrode, and lowering of sample volume will eliminate this dilution step. Recovery experiments were performed by calibrating the thread-based ISEs, then placing them in known concentrations of SUX in 20% urine. The electrodes were allowed to stabilize for 2 min, and the 10 s emf average was taken. Using the calibration, the SUX concentration was obtained, and a recovery value was calculated.

2.5. Data Analysis

The limit of detection (LOD) is mathematically calculated as the intersection of the Nernstian and non-Nernstian portions of the calibration curve. The selectivity coefficient for the primary ion (SUX) over the interfering ion $k_{i,j}^{pot}$ with FIM measurements was calculated [54]:

$$log(k_{i,j}^{pot}) = log\left(\frac{a_i(DL)}{a_j(BG)^{\frac{z_i}{z_j}}}\right), \tag{1}$$

where $a_i(DL)$ represents the SUX ion activity at the LOD and $a_j(BG)$ shows the activity of the interfering ion when none of the primary ion is present. The charges of SUX and the interfering ion are represented with z_i and z_j respectively. Activity and activity coefficient are calculated using the extended Debye–Hückel equation, assuming the ionic strength is very low (<10 mM) [55,56].

3. Results and Discussion

We first characterized the potentiometric sensing membrane for measurement of SUX. We then integrated this sensing membrane into a portable and compact yarn-based electrode, and developed a solid-state SUX electrochemical sensor. The sensor's performance was validated in spiked human urine samples.

3.1. Design and Operating Principle

Potentiometry is an electrochemical detection technique based on an ion's charge. Potentiometric sensing consists of a reference electrode that provides a sample-independent electrical potential and a working electrode (ion-selective electrode). An ion-selective

membrane (ISM) was used to select for a particular ion, SUX in this case. The ISM thermodynamically favors interaction with SUX ions due to (i) SUX's lipophilic nature and (ii) addition of calixarene-based ionophore that interacts with quaternary ammoniums. Hydrophobic ionic sites (molecules with an opposing charge, TFPB in this application) spiked into the polymer membrane provide the negative counterion to establish a constant concentration of SUX in the ISM. Calix[4]arene was selected for the ionophore due to its affinity for tetramethyl amine groups, of which SUX has two (Figure 1B) [39]. The ionic site NaTFPB was chosen for its anion's negative charge and high hydrophobicity [40,57]. While the ISM's bulk material remains electroneutral, the charge separation of SUX and its counter anion (chloride, in this study) at the ISM-sample phase boundary generates an electrical potential proportional to the activity of SUX [40]. When connected as a circuit, this ISM-sample boundary potential affects the voltage readout (traditionally referred to as electromotive force, *emf*). If all other boundary potentials are maintained constant, the *emf* will change in proportion to the activity of SUX within electrode's linear range. We expect the Nernst equation to predict the

$$emf$$

value of these ISEs [54].

$$emf = E_i^0 + \frac{RT}{z_i F} ln(a_i + \sum k_{i,j}^{pot} a_j^{\frac{z_i}{z_j}}),\tag{2}$$

where R, F, and T represent the universal gas constant, Faraday constant, and temperature in kelvins. E_i^0 represents the sum of all other contributing boundary potentials and must be constant for ion-selective potentiometric measurements to work properly. It then follows that a ten-fold change in SUX activity should result in a theoretical 29.6 mV *emf* difference.

3.2. Characterization of the SUX Sensing Membrane

To first validate that the potentiometric determination of SUX in urine is possible, we developed traditional potentiometric sensors with a liquid inner-filling solution. We dissolved all sensing components in THF, and casted the sensing membrane. This membrane was cut and pasted onto a Tygon tube, back filled with the inner-filling solution as detailed in the experimental section. This design enabled us to validate the performance of the sensing membrane separate from the construction of the portable sensor. In SUXCl$_2$ solution, the conventional ISEs (n = 5) demonstrated an LOD of 0.12 μM and a response of 29.3 mV/decade (Figure 3, Table 1). This is in line with what we expect for the response to the divalent SUX cation. The electrodes drifted -50.5 ± 60 μV/min over 30 min and reported an E^0 of 141 ± 3 mV. The stability and reproducibility are expected from these conventional electrodes and is due to the very stable nature of the Ag/AgCl-inner filling solution-ISM interfaces.

We utilized a calix[4]arene ionophore for selective detection of SUX. Prior work by us and others showed that the calixarenes, specifically calix[4]arene, show strong binding with quaternary ammoniums and act as an ionophore for other ions with similar chemical structures (acetylcholine and choline) [18,39,48,58]. While prior work showed that a calix[4]arene ionophore has the optimum ring cavity size, and exhibits the highest binding to choline and acetylcholine, we validated this for SUX as well. We compared binding strength for calix[4]arene (CX4) vs. calix[6]arene (CX6) using a reference ion for comparison, and a well-established method of validating facilitated ion transfer to the sensing membrane by the ionophore [26,39,48,59]. Figure 4 shows the *emf* of the electrodes in 10 mM tetrabutylammonium (Bu$_4$N$^+$), and in 10 mM SUX. The electrodes were not conditioned in Bu$_4$N$^+$, and the measurement was completed over a one-minute exposure to Bu$_4$N$^+$ to avoid trans-membrane fluxes and complete ion exchange in the sensing membrane. Bu$_4$N$^+$ was selected as a non-interacting reference ion since the large size of the ion makes it unfit for the calixarene cavity size. As shown in Figure 4, the CX4 shows the smallest *emf*

difference between SUX and Bu_4N^+, confirming facilitated ion transfer and ionophore-SUX interaction in the sensing membrane.
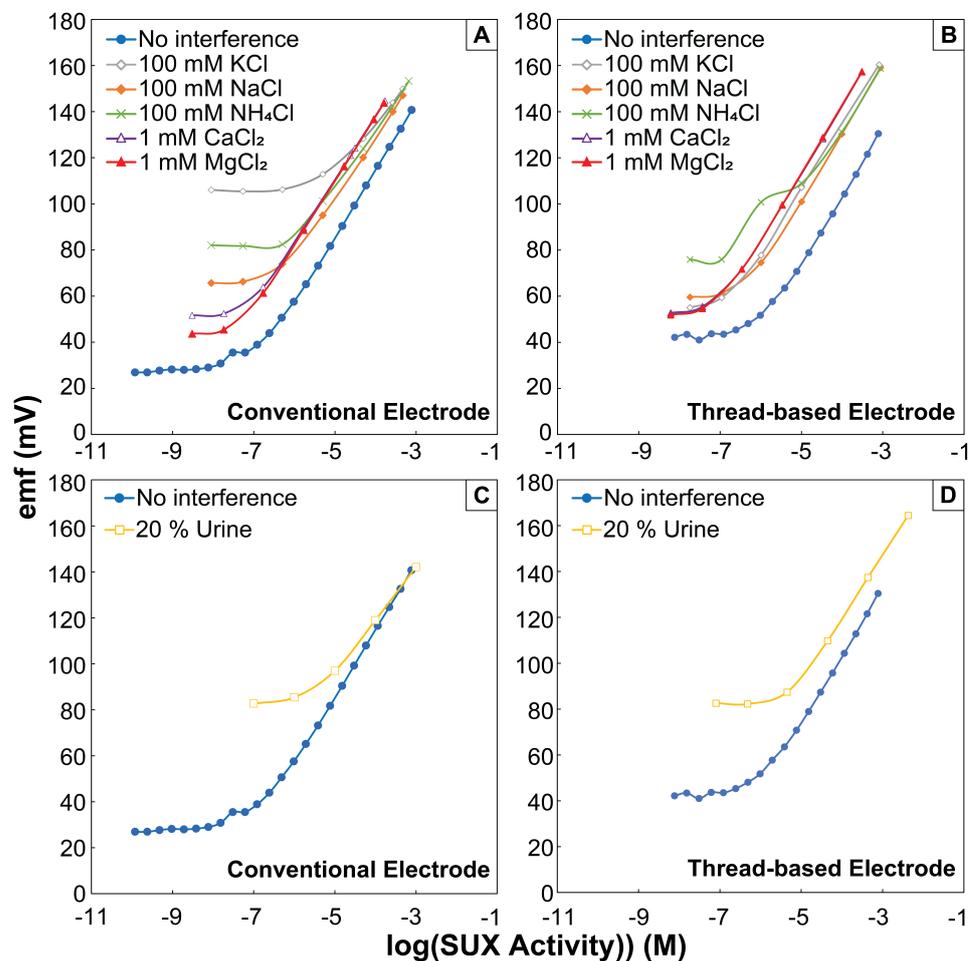

Figure 3. The response curves for (**A**,**C**) conventional ISEs and (**B**,**D**) the thread-based ISEs in the presence of a fixed concentration of interfering cations. (**A**,**B**) The interfering inorganic salts caused LODs to increase in both conventional ISE and thread-based ISE systems. (**C**,**D**) Unknown urine content caused larger increases in LOD in both systems.
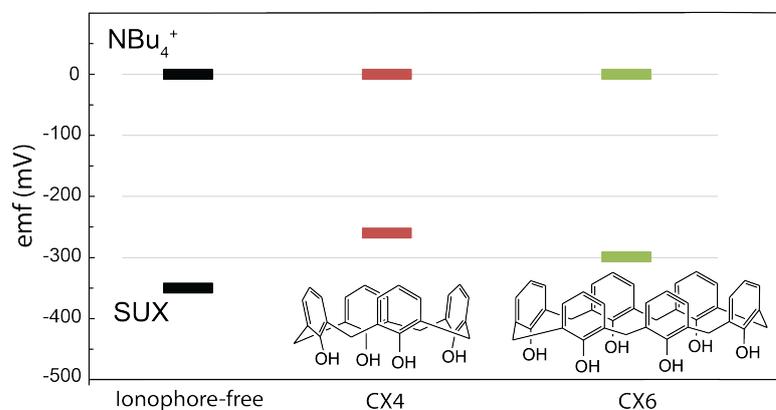

Figure 4. The differences in the *emf* of the SUX ISE for 10 mM SUX solution with respect to 10 mM Bu_4N^+ (black trace shows an ionophore-free sensing membrane, red trace shows the CX4 ionophore in the sensing membrane, and the green trace shows the CX6 ionophore in the sensing membrane).

After confirming that CX4 ionophore facilitates SUX transfer to the sensing membrane, we quantified selectivity against common interfering ions present in urine in large concentrations. We attempted quantifying selectivity using the established separate solution method [54], but could not proceed with this method since we did not observe Nernstian slope for interfering ions. We utilized the fixed interference method for quantifying the selectivity coefficient [54]. In this method, the limit of detection is measured in the presence of interfering ions, and the selectivity coefficient is calculated via Equation (1). We adjusted the concentration of the interfering ion to make sure a Nernstian response range for SUX was still achieved. Table 1 shows the calculated selectivity coefficients. Urine contains a plethora of ions and organic molecules that can interfere with the selectivity and detection limit of the conventional ISEs [60]. To confirm the selective determination of SUX in a complex urine environment, we spiked SUX in 20% pooled human urine, and showed that the sensor still exhibited Nerstian behavior (Figure 3C). The LOD increased from 0.12 μM in deionized water to 4.21 μM in pooled urine. This increase in LOD is expected due to the increase in the baseline signal coming from the large ionic background in urine.

Table 1. The interference of ionic compounds on SUX detection using CX4-conventional ISEs.

Interfering Solution	Limit of Detection (μM)	Response (mV/decade)	$log(k_{i,j}^{pot})$
None	0.12	29.3 ± 1	–
20% Urine	4.21	23.1 ± 2	–
100 mM KCl	7.73	24.5 ± 2	−2.79
100 mM NaCl	0.08	28.9 ± 1	−3.78 *
100 mM NH$_4$Cl	1.66	27.3 ± 3	−3.46
100 mM CaCl$_2$	0.10	28.5 ± 2	−3.70 *
100 mM MgCl$_2$	0.06	28.0 ± 2	−3.97 *

* These are maximum selectivity coefficients; conclusions cannot be drawn due to a smaller-than-one order of magnitude difference in LOD compared to the non-interfering case.

3.3. Development of the Thread-Based SUX Sensor

While conventional ISEs show a good performance for SUX detection, the need for an inner filling solution complicates electrode maintenance and use. Solid-state electrodes do not require an inner filling solution, which makes usage and maintenance simpler, while unlocking new material and form-factor possibilities. Thread has been shown to be a suitable substrate for solid-state ISEs for detection K^+, Na^+, and Ca^{2+} [20]. Thread is an excellent substrate because it (i) has a high surface area-to-volume ratio, (ii) is light and has excellent mechanical properties (particularly tensile strength and flexibility), (iii) does not require microfabrication techniques, and (iv) can support a conductive ink and ISM on the same substrate [20]. Figure 2 shows the fabrication of the thread-based sensors. A cotton yarn was coated with a hydrophobic carbon black ink made with the same polymer and plasticizer as the ISM. This helps stabilize the electrode-membrane interface and improves adhesion of the sensing membrane to the ink-coated yarn. The high surface area and porosity of carbon black ensures high signal stability for the solid-contact ISE [19]. Cross-sectional SEM images of of the completed electrode shows full impregnation of the carbon black into the cotton yarn, as well as excellent physical connection between the electrode and the ISM (Figure 2).

The CX4-thread-based ISEs (n = 4) in SUXCl$_2$ demonstrated a linear response range of 1 mM to 3.12 μM (LOD of 1.04 μM), with a theoretically-expected Nernstian slope of 29.7 ± 0.1 mV/decade. The CX4-thread-based ISEs demonstrated a 17.6 ± 20 μV/min drift over 30 min (unconditioned fresh dry-stored sensors) with an average E^0 of 155 ± 10 mV. The large standard deviation with E^0 indicates poor out-of-the-box reproducibility of these sensors, likely due to the crude nature by which the 25% CB ink was impregnated onto the yarn and inconsistency in the material of the yarn itself. This means that each sensor needs to be calibrated before use, which is inconvenient for in-field use. A more refined industrialized process with a more uniform thread and a more precise mechanism to cut the

yarn to length could reduce variability between sensors. However, the Nernstian response demonstrated a near-theoretical slope with low standard deviation, indicating that each sensor is reliable within its LOD after it is properly calibrated.

Future work on thread-based ISEs should take these challenges into account and focus on developing calibration-free ISEs. Although response time was not explicitly evaluated, the thread-based ISEs demonstrate a rapid response time in the order of seconds (Figure 5 inlay). While our experiments continued with 2 min equilibration times before measurements, this time could be significantly shortened. The sensor demonstrates an acceptable LOD with a Nernstian response and is stable over 30 min. Because the intended field-test use case will occur over a few minutes, not hours, this test period is acceptable. The extended use of solid-state ISEs in aqueous solutions may result in the formation of a water layer. This water layer acts as a reservoir for solution, causing equilibration problems and drift in *emf* as dilutions are performed for different concentrations [43]. Given that the intended use for this sensor was rapid on-site testing and disposing of the sensor afterwards, water layer formation was not studied.
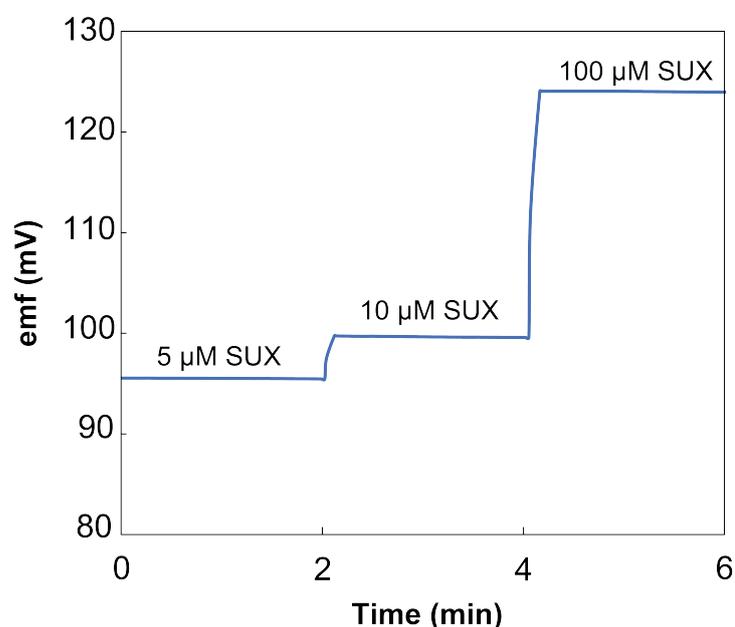

Figure 5. The *emf* traces from recovery experiments where thread-based ISEs were exposed to 5, 10, and 100 μM concentrations of SUX in 20% urine.

In 20% urine, the thread-based ISEs demonstrated a 4.27 μM LOD and response of 27.6 ± 0.3 mV/decade. This LOD is satisfactory for the determination of SUX in urine samples. Prior work showed that 5.7–56.9 μg/mL $SUXCl_2$ can be found in urine of patients under SUX anesthesia, 40 to 70 min post injection [7]. This value is equivalent to 16 μM to 157 μM $SUXCl_2$, which will be detectable in 20% urine with the thread-based

SUX electrodes. Selectivity towards individual cations was quantified using the fixed interference method (similar to the conventional ISEs). Table 2 shows the values and Figure 3B,D show the electrode response in the presence of interfering ions. It is important to note that the intercepts of the conventional ISEs and the thread-based ISEs cannot be directly compared. The two different types establish their internal references differently (conventional ISEs through the Ag/AgCl wire and chloride in the inner filling solution, and the thread-based ISEs through the capacitive interface between the carbon black and the sensing membrane), and will result in different E^0 in the calibration equation.

Table 2. The interference of ionic compounds on SUX detection using CX4-thread-based ISEs.

Interfering Solution	Limit of Detection (µM)	Response (mV/decade)	$log(k_{i,j}^{pot})$
None	1.04	29.7 ± 0.1	–
20% Urine	4.27	27.6 ± 0.3	–
100 mM KCl	0.23	27.9 ± 2	−4.32 *
100 mM NaCl	0.53	29.9 ± 0.2	−3.95 *
100 mM NH$_4$Cl	1.24	29.1 ± 0.4	−3.58 *
100 mM CaCl$_2$	0.13	29.5± 0.7	−3.60 *
100 mM MgCl$_2$	0.12	29.7 ± 0.1	−3.62 *

* These are maximum selectivity coefficients; conclusions cannot be drawn due to a smaller-than-one order of magnitude difference in LOD compared to the non-interfering case.

3.4. SUX Recovery

After confirming the selectivity and sensitivity of the portable yarn-based SUX sensors, we tested the accuracy of measurements taken with this new tool. After fabricating and calibrating the thread-based ISEs, we placed them into 20% urine samples containing 5, 10, and 100 µM concentrations of SUXCl$_2$ (Figure 5). We chose these concentrations to reflect the expected SUX range in urine post injection. The recovery value of SUX was calculated by converting the recorded *emf* of the sensors in sample solutions to SUX concentration using the calibration equation of the sensors. They reported average recovery values of 94.1 ± 0.2%, 96.9 ± 0.4%, and 99.9 ± 0.3%, respectively. The recovery value is highest for the 100 µM concentration since it is the furthest within the linear range, and the lowest recovery value was found near the LOD. These experiments demonstrate the expected use case for the thread-based ISEs.

The sensors show acceptable accuracy in quantifying SUXCl$_2$ in a 20% urine solution within the linear range with low variability.

4. Conclusions

In this work, we have developed a thread-based ISE for the detection of SUX in human urine. The thread-based ISE demonstrates an acceptable LOD for detecting evidence of SUX in urine. It also demonstrates excellent stability in the short-term timeframe of forensic analysis and high selectivity against nonorganic cations.

The thread-based ISE is not intended to replace high-definition HPLC/MS methods. However, it can aid in rapid decision-making for these longer, more elaborate tests. The relative simplicity of fabrication, storage, and utilization of the device shows potential for large-scale deployment by law enforcement. Our thread-based SUX sensor is capable of rapid on-site analysis which is advantageous for SUX measurement due to the instability of SUX, and the potential impact on longterm storage in compromising the sample. In conjunction with the development of smaller, low-cost reference electrodes, this would make potentiometric sensors inexpensive, portable, and simple enough to be used by untrained persons. The application of these systems to a wide range of analytes could contribute to a new field of rapid on-site forensic devices that could revolutionize the way that drug and poison sensing is performed. Beyond the forensic use-case, such a system can be mass-marketed for healthcare screening and monitoring, food safety, agricultural analysis, and more.

Future improvements are needed for the commercialization of this potentiometric SUX platform. The reproducibility of the thread-based ISEs must be improved at the manufacturing and industry levels. Further improvement of sensor selectivity would be advantageous, perhaps through the development of better ionophores, or the use of fluorous-phase sensing matrices [61–63]. This selectivity enhancement enables the detection of SUX at nanomolar levels, and opens up the application of the sensor for tissue analysis. The need to pre-calibrate each sensor increases the complexity of the system and makes utilizing the sensors more difficult. Future work should also focus on developing calibration-free thread-based potentiometric sensors.

Author Contributions: Conceptualization, V.O., M.K.A.E.-R. and M.P.S.M.; methodology, V.O. and M.P.S.M.; validation, V.O., F.A., N.R.C. and Z.X.; formal analysis, V.O.; investigation, V.O., N.R.C. and Z.X.; resources, V.O. and M.P.S.M.; writing—original draft preparation, V.O.; writing—review and editing, M.P.S.M. and M.K.A.E.-R.; visualization, V.O.; supervision, M.P.S.M. and V.O.; project administration, V.O.; funding acquisition, M.P.S.M. All authors have read and agreed to the published version of the manuscript.

Institutional Review Board Statement: Not Applicable.

Informed Consent Statement: Not Applicable.

Data Availability Statement: No external data sets were used in this project.

Conflicts of Interest: The authors declare no conflict of interest. The funders had no role in the design of the study; in the collection, analyses, or interpretation of data; in the writing of the manuscript, or in the decision to publish the results.

References

1. Kuepper, U.; Musshoff, F.; Madea, B. Succinylmonocholine analytics as an example for selectivity problems in high-performance liquid chromatography/tandem mass spectrometry, and resulting implications for analytical toxicology. *Rapid Commun. Mass Spectrom.* **2008**, *22*, 1965–1970. [CrossRef] [PubMed]

2. Pitts, N.; Deftereos, D.; Mitchell, G. Determination of succinylcholine in plasma by high-pressure liquid chromatography with electrochemical detection. *Br. J. Anaesth.* **2000**, *85*, 592–598. [CrossRef]

3. Kuepper, U.; Musshoff, F.; Madea, B. Fully validated isotope dilution HPLC-MS/MS method for the simultaneous determination of succinylcholine and succinylmonocholine in serum and urine samples. *J. Mass Spectrom.* **2008**, *43*, 1344–1352. [CrossRef] [PubMed]

4. Van der Zee, E.A.; Platt, B.; Riedel, G. Acetylcholine: Future research and perspectives. *Behav. Brain Res.* **2011**, *221*, 583–586. [CrossRef] [PubMed]

5. Rubinstein, H.M.; Rosenberg, M.K.; Bolgla, J.H.; Cohen, B.M. Prolonged Apnea after Administration of Succinylcholine. *N. Engl. J. Med.* **1960**, *262*, 1107–1111. [CrossRef]

6. Geyer, B.C.; Larrimore, K.E.; Kilbourne, J.; Kannan, L.; Mor, T.S. Reversal of Succinylcholine Induced Apnea with an Organophosphate Scavenging Recombinant Butyrylcholinesterase. *PLoS ONE* **2013**, *8*, e59159. [CrossRef]

7. Kuepper, U.; Herbstreit, F.; Peters, J.; Madea, B.; Musshoff, F. Degradation and elimination of succinylcholine and succinylmonocholine and definition of their respective detection windows in blood and urine for forensic purposes. *Int. J. Leg. Med.* **2012**, *126*, 259–269. [CrossRef]

8. Kuepper, U.; Musshoff, F.; Hilger, R.A.; Herbstreit, F.; Madea, B. Pharmacokinetic Properties of Succinylmonocholine in Surgical Patients. *J. Anal. Toxicol.* **2011**, *35*, 302–311. [CrossRef]

9. Roy, J.J.; Boismenu, D.; Gao, H.; Mamer, O.A.; Varin, F. Measurement of succinylcholine concentration in human plasma by electrospray tandem mass spectrometry. *Anal. Biochem.* **2001**, *290*, 238–244. [CrossRef]

10. Lagerwerf, A.; Vanlinthout, L.; Vree, T. Rapid determination of succinylcholine in human plasma by high-performance liquid chromatography with fluorescence detection. *J. Chromatogr.* **1991**, *570*, 390–395. [CrossRef]

11. Xing, J.; Li, W.; Tong, F.; Liang, Y.; He, G.; Zhou, Y. Three homicides with darts tainted with succinylcholine: Autopsy and toxicology. *Int. J. Leg. Med.* **2016**, *130*, 1541–1545. [CrossRef]

12. Guo, W.; Luo, G.; Wang, H.; Meng, X. Homicide by Sch from a syringe-like dart ejected by a compound crossbow. *J. Forensic Leg. Med.* **2014**, *30*, 25–28. [CrossRef] [PubMed]

13. Yorker, B.C.; Kizer, K.W.; Lampe, P.; Forrest, A.; Lannan, J.M.; Russell, D.A. Serial Murder by Healthcare Professionals. *J. Forensic Sci.* **2006**, *51*, 1362–1371. [CrossRef]

14. Maeda, H.; Fujita, M.Q.; Zhu, B.L.; Ishidam, K.; Oritani, S.; Tsuchihashi, H.; Nishikawa, M.; Izumi, M.; Matsumoto, F. A case of serial homicide by injection of succinylcholine. *Med. Sci. Law* **2000**, *40*, 169–174. [CrossRef]

15. Stevens, H.; Moffat, A. A Rapid Screening Procedure for Quaternary Ammonium Compounds in Fluids and Tissues with Special Reference to Suxamethonium (Succinylcholine). *J. Forensic Sci. Soc.* **1974**, *14*, 141–148. [CrossRef]

16. Cheong, Y.H.; Ge, L.; Lisak, G. Highly reproducible solid contact ion selective electrodes: Emerging opportunities for potentiometry—A review. *Anal. Chim. Acta* **2021**, *1162*, 338304. [CrossRef]

17. De Rycke, E.; Stove, C.; Dubruel, P.; De Saeger, S.; Beloglazova, N. Recent developments in electrochemical detection of illicit drugs in diverse matrices. *Biosens. Bioelectron.* **2020**, *169*, 112579. [CrossRef] [PubMed]

18. ElDin, N.B.; El-Rahman, M.K.A.; Zaazaa, H.E.; Moustafa, A.A.; Hassan, S.A. Microfabricated potentiometric sensor for personalized methacholine challenge tests during the COVID-19 pandemic. *Biosens. Bioelectron.* **2021**, *190*, 113439. [CrossRef]

19. Hu, J.; Stein, A.; Bühlmann, P. Rational design of all-solid-state ion-selective electrodes and reference electrodes. *TrAC Trends Anal. Chem.* **2016**, *76*, 102–114. [CrossRef]

20. Mousavi, M.P.S.; Ainla, A.; Tan, E.K.W.; El-Rahman, M.K.A.; Yoshida, Y.; Yuan, L.; Sigurslid, H.H.; Arkan, N.; Yip, M.C.; Abrahamsson, C.K.; et al. Ion sensing with thread-based potentiometric electrodes. *Lab Chip* **2018**, *18*, 2279–2290. . [CrossRef]

21. Rousseau, C.R.; Bühlmann, P. Calibration-free potentiometric sensing with solid-contact ion-selective electrodes. *TrAC Trends Anal. Chem.* **2021**, *140*, 116277. [CrossRef]

22. Shao, Y.; Ying, Y.; Ping, J. Recent advances in solid-contact ion-selective electrodes: Functional materials, transduction mechanisms, and development trends. *Chem. Soc. Rev.* **2020**, *49*, 4405–4465. . [CrossRef]

23. Teymourian, H.; Parrilla, M.; Sempionatto, J.R.; Montiel, N.F.; Barfidokht, A.; Van Echelpoel, R.; De Wael, K.; Wang, J. Wearable Electrochemical Sensors for the Monitoring and Screening of Drugs. *ACS Sens.* **2020**, *5*, 2679–2700. [CrossRef] [PubMed]

24. Vasantham, S.; Alhans, R.; Singhal, C.; Nagabooshanam, S.; Nissar, S.; Basu, T.; Ray, S.C.; Wadhwa, S.; Narang, J.; Mathur, A. Paper based point of care immunosensor for the impedimetric detection of cardiac troponin I biomarker. *Biomed. Microdevices* **2020**, *22*, 6. [CrossRef] [PubMed]

25. Xiao, G.; Ju, J.; Lu, H.; Shi, X.; Wang, X.; Wang, W.; Xia, Q.; Zhou, G.; Sun, W.; Li, C.M.; et al. A Weavable and Scalable Cotton-Yarn-Based Battery Activated by Human Sweat for Textile Electronics. *Adv. Sci.* **2022**, *9*, e2103822. [CrossRef]

26. Banks, M.; Amirghasemi, F.; Mitchell, E.; Mousavi, M.P.S. Home-Based Electrochemical Rapid Sensor (HERS): A Diagnostic Tool for Bacterial Vaginosis. *Sensors* **2023**, *23*, 1891. [CrossRef] [PubMed]

27. Bhattacharjee, M.; Nemade, H.B.; Bandyopadhyay, D. Nano-enabled paper humidity sensor for mobile based point-of-care lung function monitoring. *Biosens. Bioelectron.* **2017**, *94*, 544–551. [CrossRef]

28. Hu, J.; Wang, S.; Wang, L.; Li, F.; Pingguan-Murphy, B.; Lu, T.J.; Xu, F. Advances in paper-based point-of-care diagnostics. *Biosens. Bioelectron.* **2014**, *54*, 585–597. [CrossRef] [PubMed]

29. Li, H.; Wang, W.; Lv, Q.; Xi, G.; Bai, H.; Zhang, Q. Disposable paper-based electrochemical sensor based on stacked gold nanoparticles supported carbon nanotubes for the determination of bisphenol A. *Electrochem. Commun.* **2016**, *68*, 104–107. [CrossRef]

30. Madhu, S.; Ramasamy, S.; Magudeeswaran, V.; Manickam, P.; Nagamony, P.; Chinnuswamy, V. SnO_2 nanoflakes deposited carbon yarn-based electrochemical immunosensor towards cortisol measurement. *J. Nanostruct. Chem.* **2022**, *13*, 115–127. [CrossRef]

31. Wang, L.; Lu, J.; Li, Q.; Li, L.; He, E.; Jiao, Y.; Ye, T.; Zhang, Y. A Core–Sheath Sensing Yarn-Based Electrochemical Fabric System for Powerful Sweat Capture and Stable Sensing. *Adv. Funct. Mater.* **2022**, *32*, 2200922. [CrossRef]

32. Wang, C.C.; Hennek, J.W.; Ainla, A.; Kumar, A.A.; Lan, W.J.; Im, J.; Smith, B.; Zhao, M.; Whitesides, G.M. A Paper-Based "Pop-up" Electrochemical Device for Analysis of Beta-Hydroxy-butyrate. *Anal. Chem.* **2016**, *88*, 6326–6333. [CrossRef]

33. Wang, Y.; Zhang, Y.; Wang, Y.; Zhu, R.; Chen, Y.; Liu, X.; Xu, J.; Li, M.; Wang, D. Urea Detection of Electrochemical Transistor Sensors based on Polyanline (PANI)/MWCNT/Cotton Yarns. *Electroanalysis* **2021**, *33*, 2406–2416. [CrossRef]

34. Scordo, G.; Moscone, D.; Palleschi, G.; Arduini, F. A reagent-free paper-based sensor embedded in a 3D printing device for cholinesterase activity measurement in serum. *Sens. Actuators B Chem.* **2018**, *258*, 1015–1021. [CrossRef]

35. Mujawar, L.H.; Felemban, A.A.; El-Shahawi, M.S. Hexamethyldisilazane Modified Paper as an Ultra-sensitive Platform for Visual Detection of Hg^{2+}, Co^{2+}, Zn^{2+} and the Application to Semi-quantitative Determination of Hg^{2+} in Wastewater. *Anal. Sci.* **2016**, *32*, 491–497. [CrossRef]

36. Liu, M.M.; Lian, X.; Liu, H.; Guo, Z.Z.; Huang, H.H.; Lei, Y.; Peng, H.P.; Chen, W.; Lin, X.H.; Liu, A.L.; et al. A colorimetric assay for sensitive detection of hydrogen peroxide and glucose in microfluidic paper-based analytical devices integrated with starch-iodide-gelatin system. *Talanta* **2019**, *200*, 511–517. [CrossRef]

37. Gu, Z.; Zhao, M.; Sheng, Y.; Bentolila, L.A.; Tang, Y. Detection of Mercury Ion by Infrared Fluorescent Protein and Its Hydrogel-Based Paper Assay. *Anal. Chem.* **2011**, *83*, 2324–2329. [CrossRef] [PubMed]

38. Lee, J.; Ko, S.; Kwon, C.H.; Lima, M.D.; Baughman, R.H.; Kim, S.J. Carbon Nanotube Yarn-Based Glucose Sensing Artificial Muscle. *Small* **2016**, *12*, 2085–2091. [CrossRef] [PubMed]

39. Mousavi, M.P.S.; Abd El-Rahman, M.K.; Mahmoud, A.M.; Abdelsalam, R.M.; Bühlmann, P. In Situ Sensing of the Neurotransmitter Acetylcholine in a Dynamic Range of 1 nM to 1 mM. *ACS Sens.* **2018**, *3*, 2581–2589. [CrossRef]

40. Bühlmann, P.; Chen, L.D. Ion-Selective Electrodes with Ionophore-Doped Sensing Membranes. *Supramol. Chem.* **2012**, *5*, 2539. [CrossRef]

41. Parrilla, M.; De Wael, K. Wearable Self-Powered Electrochemical Devices for Continuous Health Management. *Adv. Funct. Mater.* **2021**, *31*, 2107042. [CrossRef]

42. Zdrachek, E.; Bakker, E. Potentiometric Sensing. *Anal. Chem.* **2021**, *93*, 72–102. [CrossRef]

43. Veder, J.P.; De Marco, R.; Clarke, G.; Chester, R.; Nelson, A.; Prince, K.; Pretsch, E.; Bakker, E. Elimination of undesirable water layers in solid-contact polymeric ion-selective electrodes. *Anal. Chem.* **2008**, *80*, 6731–6740. [CrossRef] [PubMed]

44. Bieg, C.; Fuchsberger, K.; Stelzle, M. Introduction to polymer-based solid-contact ion-selective electrodes—Basic concepts, practical considerations, and current research topics. *Anal. Bioanal. Chem.* **2017**, *409*, 45–61. [CrossRef]

45. Guzinski, M.; Jarvis, J.M.; Pendley, B.D.; Lindner, E. Equilibration Time of Solid Contact Ion-Selective Electrodes. *Anal. Chem.* **2015**, *87*, 6654–6659. [CrossRef]

46. Nikolskii, B.P.; Materova, E.A. Solid Contact in Membrane Ion-Selective Electrodes. In *Ion-Selective Electrode Reviews*; Thomas, J.D.R., Ed.; Elsevier: Amsterdam, The Netherlands, 1985; Volume 7, pp. 3–39. [CrossRef]

47. Tutulea-Anastasiu, M.D.; Wilson, D.; Del Valle, M.; Schreiner, C.M.; Cretescu, I. A Solid-Contact Ion Selective Electrode for Copper(II) Using a Succinimide Derivative as Ionophore. *Sensors* **2013**, *13*, 4367–4377. [CrossRef] [PubMed]

48. Abd El-Rahman, M.K.; Mazzone, G.; Mahmoud, A.M.; Sicilia, E.; Shoeib, T. Novel choline selective electrochemical membrane sensor with application in milk powders and infant formulas. *Talanta* **2021**, *221*, 121409. [CrossRef]

49. Garima.; Sachdev, A.; Matai, I. An electrochemical sensor based on cobalt oxyhydroxide nanoflakes/reduced graphene oxide nanocomposite for detection of illicit drug-clonazepam. *J. Electroanal. Chem.* **2022**, *919*, 116537. [CrossRef] [PubMed]

50. Goodchild, S.A.; Hubble, L.J.; Mishra, R.K.; Li, Z.; Goud, K.Y.; Barfidokht, A.; Shah, R.; Bagot, K.S.; McIntosh, A.J.S.; Wang, J. Ionic Liquid-Modified Disposable Electrochemical Sensor Strip for Analysis of Fentanyl. *Anal. Chem.* **2019**, *91*, 3747–3753. [CrossRef]

51. Klimuntowski, M.; Alam, M.M.; Singh, G.; Howlader, M.M.R. Electrochemical Sensing of Cannabinoids in Biofluids: A Noninvasive Tool for Drug Detection. *ACS Sens.* **2020**, *5*, 620–636. [CrossRef]

52. Parrilla, M.; Joosten, F.; De Wael, K. Enhanced electrochemical detection of illicit drugs in oral fluid by the use of surfactant-mediated solution. *Sens. Actuators B Chem.* **2021**, *348*, 130659. [CrossRef]

53. Shaw, L.; Dennany, L. Applications of electrochemical sensors: Forensic drug analysis. *Curr. Opin. Electrochem.* **2017**, *3*, 23–28. [CrossRef]

54. Bakker, E.; Pretsch, E.; Bühlmann, P. Selectivity of Potentiometric Ion Sensors. *Anal. Chem.* **2000**, *72*, 1127–1133. [CrossRef]

55. Skoog, D.; West, D.; Holler, F.; Crouch, S. *Fundamentals of Analytical Chemistry*; Cengage Learning: Boston, MA, USA, 2013. [CrossRef]

56. Shaukat, S.; Fedotova, M.V.; Kruchinin, S.E.; Bešter-Roga, M.; Podlipnik, B.-R.; Buchner, R. Hydration and ion association of aqueous choline chloride and chlorocholine chloride. *Phys. Chem. Chem. Phys. PCCP* **2019**, *21*, 197–198. [CrossRef]

57. Bühlmann, P.; Pretsch, E.; Bakker, E. Carrier-Based Ion-Selective Electrodes and Bulk Optodes. 2. Ionophores for Potentiometric and Optical Sensors. *Chem. Rev.* **1998**, *98*, 1593–1688.

58. El-Rahman, M.K.A.; Mahmoud, A.M. A novel approach for spectrophotometric determination of succinylcholine in pharmaceutical formulation via host–guest complexation with water-soluble p-sulfonatocalixarene. *RSC Adv.* **2015**, *5*, 62469–62476. [CrossRef]

59. Ceresa, A.; Pretsch, E. Determination of formal complex formation constants of various Pb^{2+} ionophores in the sensor membrane phase. *Anal. Chim. Acta* **1999**, *395*, 41–52. [CrossRef]

60. Sarigul, N.; Korkmaz, F.; Kurultak, İ. A New Artificial Urine Protocol to Better Imitate Human Urine. *Sci. Rep.* **2019**, *9*, 20159. [CrossRef]

61. Boswell, P.G.; Bühlmann, P. Fluorous Bulk Membranes for Potentiometric Sensors with Wide Selectivity Ranges: Observation of Exceptionally Strong Ion Pair Formation. *J. Am. Chem. Soc.* **2005**, *127*, 8958–8959. [CrossRef]

62. Chen, X.V.; Mousavi, M.P.; Bühlmann, P. Fluorous-Phase Ion-Selective pH Electrodes: Electrode Body and Ionophore Optimization for Measurements in the Physiological pH Range. *ACS Omega* **2020**, *5*, 13621–13629. [CrossRef] [PubMed]

63. Boswell, P.G.; Szíjjártó, C.; Jurisch, M.; Gladysz, J.A.; Rábai, J.; Bühlmann, P. Fluorophilic Ionophores for Potentiometric pH Determinations with Fluorous Membranes of Exceptional Selectivity. *Anal. Chem.* **2008**, *80*, 2084–2090. [CrossRef]